ACS PHYSICAL CHEMISTRY Au
AN OPEN ACCESS JOURNAL OF THE AMERICAN CHEMICAL SOCIETY

Open Access
This article is licensed under CC-BY-NC-ND 4.0

pubs.acs.org/physchemau
Letter

Conductance Measurements of Polar Molecules in a Nonconducting Solvent

Clark Otey,[‖] Mukund Sharma,[‖] Jazmine Prana, Thomas M. Czyszczon-Burton, Alejandro Hernandez, María Camarasa-Gómez,* Daniel Hernangómez-Pérez,* and Michael S. Inkpen*

Cite This: https://doi.org/10.1021/acsphyschemau.5c00021
Read Online

ACCESS | Metrics & More | Article Recommendations | Supporting Information

ABSTRACT: Solution-based single-molecule conductance measurements of α,ω-bis(carboxylic acids) are conveniently performed using a high-boiling-point nonconducting ethereal solvent. First-principles calculations support experimental observations that linear oligoalkanes exhibit the expected exponential decay of conductance with length, whereas junctions comprising cyclic bridge hydrocarbons of different lengths and/or structures exhibit a similar conductance.

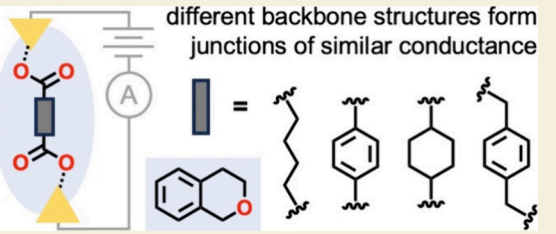

KEYWORDS: *carboxylic acids, single-molecule junctions, isochroman, tunnel coupling, DFT-NEGF, molecular electronics*

Downloaded via 150.241.32.208 on April 28, 2025 at 09:00:58 (UTC).
See https://pubs.acs.org/sharingguidelines for options on how to legitimately share published articles.

A central goal of molecular electronics is to develop functional molecular-scale components that may one day serve as nanoscale electronic circuit elements.[1] To drive future advances, a deeper understanding of the complex interplay between electrode, linker group, and molecular backbone properties and the impact of this relationship on charge transport through metal−molecule−metal junctions is required. We focus here on carboxylic acids, well-recognized linkers that facilitate the spontaneous formation of single-molecule junctions from aqueous solutions[2,3] or components adsorbed/deposited on surfaces (Figure 1a).[4−6] Their weakly

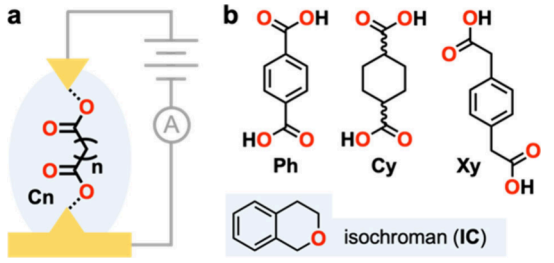

Figure 1. (a) Schematic of molecular junctions formed from linear oligoalkane α,ω-bis(carboxylic acids) bound between gold electrodes. (b) Molecular structures of cyclic α,ω-bis(carboxylic acid) junction components and isochroman, a high-boiling-point ethereal solvent.

acidic character, hydrophilicity, and reactivity have enabled studies exploring the pH-dependence of junction conductance,[3,6,7] the use of electrochemically stabilized silver, copper, and palladium electrodes,[8−10] or the reversible formation of ester-containing molecular circuits.[5] However, the capacity of bis(carboxylic acids) to generate extended hydrogen-bonding networks in the solid state[11] can limit their solubility in commonly used electrically insulating scanning tunneling microscope (STM) solvents. To date, only two single-molecule conductance studies in such solvents have been reported: one using tetradecane (TD), restricted to compounds containing a *single* carboxylic acid,[7] and one of bis(carboxylic acids) in toluene.[8]

Here we report that nonconducting organic solvents comprising oxygen functionalities can improve the solubility of polar compounds of interest, presumably by disrupting analyte−analyte intermolecular interactions. Critically, the use of isochroman (**IC**; Figure 1b) enables conductance measurements of α,ω-bis(carboxylic acids) with different backbones using uncoated[12] STM tips. These experimental studies, supported by *first-principles* calculations of model junctions, provide important new insights into the nature of charge transport across the −AuOC(O)− interfacial contact.

We perform conductance measurements using the STM-based break junction (STM-BJ) method (see the SI for more details).[13,14] This technique involves repeatedly pushing an uncoated gold tip in and out of a gold substrate while applying a voltage bias (V_{bias}) between these electrodes and measuring the current (I) as a function of the tip−substrate displacement. Step features observed in the resulting conductance ($G = I/V_{bias}$)−displacement traces correspond to the formation of Au−Au point contacts at close to integer multiples of 1 G_0 (= $2e^2/h$) and molecular junctions at lower conductance (after

Received: March 10, 2025
Revised: April 18, 2025
Accepted: April 21, 2025

ACS Publications
© XXXX The Authors. Published by American Chemical Society

the addition of a suitable analyte in solution). Thousands of these traces are compiled, without data selection, into 1D conductance and 2D conductance−displacement histograms. The resulting histogram features reveal the most probable properties of the junctions studied.

The utility of four different high-boiling-point ethereal solvents for STM-BJ studies was first evaluated using 4,4′-bipyridine (**bipy**). Two solvents are cyclic ethers: **IC** (boiling point (BP) ∼214 °C) and 2,3-dihydrobenzofuran (188 °C). The other two are acyclic ethers: dioctylether (286 °C) and cyclopentyl methyl ether (106 °C). Explicit molecular structures for these compounds are provided in Figure S1a. Each measurement provides histograms containing the characteristic two-peak feature of **bipy** junctions, corresponding to N lone pair−Au and pyridyl π−Au contact geometries,[15] indicating that these solvents do not impede junction formation (Figure S1b−e). The conductance of junctions measured in these solvents typically lie between or above those obtained from measurements in TD or 1,2,4-trichlorobenzene, further indicating these new solvents only weakly interact with the gold surface (Table S1).[16,17] The low instrument noise floor in these, and subsequent, measurements illustrate the electrically insulating nature of these solvents; no significant electrochemical currents are observed. We select **IC** for additional studies given its moderate BP and mixed aliphatic-aromatic structure, which we reason will help solubilize a wider range of compounds.

We subsequently perform conductance measurements using **IC** solutions of alkane α,ω-bis(carboxylic acids) (**C*n***, where n is the number of carbon atoms between HOC(O)- linkers; Figure 1a). We plot, in Figure 2, overlaid 1D histograms for

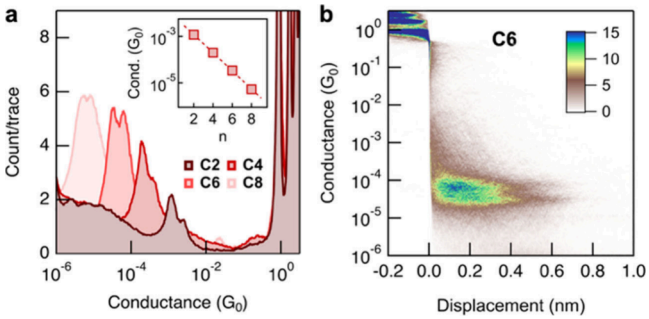

Figure 2. (a) Overlaid 1D histograms for **C*n*** measured in **IC** (V_{bias} = 250 mV, 5000 traces). Inset: plot of the experimental single-molecule conductance against n (β = 0.90/n). (b) 2D histogram for **C6**.

these diacids. All histograms contain a sharp peak feature toward lower conductance, assigned to single-molecule junctions. In each case, we also observe an additional peak or shoulder at ∼2× the conductance of the first peak, which we tentatively attribute to the formation of junctions with two molecules in parallel. These distinct features are also clearly observed in the corresponding 2D histograms and individual conductance−displacement traces (Figure 2b and S2). A semilog plot of the most probable conductance for each single-molecule junction against n shows that these values exhibit an exponential length dependence indicative of tunneling transport (Figure 2, inset). We obtain a tunneling decay constant (β) of 0.90/n and a contact conductance (G_c) of 7.2×10^{-3} G_0 from a linear fit to this data using $G = G_c \cdot \exp(-\beta n)$. This β is consistent with values obtained for other series of oligoalkanes with different linker groups, and the low G_c (e.g., relative to 4.8×10^{-2} G_0 for −SMe), attributed to the additional carbon atom in the linker group, also agrees well with previous reports.[3,7,8,18] Conductance data for all diacid junctions are provided in Table S2. Additional discussion regarding studies of ethanedioic acid (**C0**) in **IC**, and **C6** introduced using different methods, is provided in the SI.

We next evaluate the conductance of junctions formed from α,ω-bis(carboxylic acids) comprising cyclic 1,4-phenylene (**Ph**, n = 4), 1,4-cyclohexane (**Cy**, n = 4), and 1,4-xylylene (**Xy**, n = 6) backbones (for molecular structures, see Figure 1b). Here, values of n indicate the number of carbon atoms between linkers through a single branch of the backbone ring. In Figure 3a we plot overlaid 1D conductance histograms for these cyclic

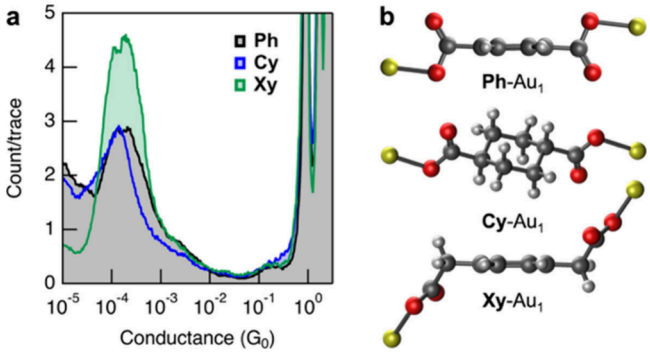

Figure 3. (a) Overlaid 1D histograms for measurements of **Ph**, **Cy**, and **Xy** in **IC** (V_{bias} = 250 mV, ≥5000 traces). (b) Au_1-cluster junction geometries that provide the highest tunnel couplings for each system.

diacids, in which we again typically observe two overlapping peaks characteristic of one and two molecular junctions. Surprisingly, while their hydrocarbon bridges differ in the number and structure (aliphatic, aromatic) of carbon atoms, these diacid junctions each exhibit a conductance within a factor of 1.1 from each other and between 60% and 68% of the conductance of **C4** (Table S2). Repeated measurements of these analytes highlight the reproducibility of this result (Figure S3a−c). Our findings contrast with the ∼10× higher conductance reported for **Ph** compared to **Xy** junctions formed using copper electrodes,[19] although the conductance data obtained for **Ph** in that study included additional peak features at lower conductance.

To provide additional insights into the electronic properties of these junctions, we turn to *first-principles* calculations based on density functional theory (DFT; see the SI for further details and extended discussion). Each contact is initially modeled in Au_1 cluster junctions using a κ^1 (O-monodentate) coordination mode. This geometry is observed in molecular structures of Au(I)−carboxylate complexes determined from single-crystal X-ray diffraction (although Ag(I) and Cu(I) complexes with κ^2 (O,O-bidentate) or bridging coordination geometries are known).[20] Given that rotations about the unconstrained and sterically unimpeded single bonds in each system (e.g., AuOC(O)-aryl) are expected to be soft degrees of freedom,[16,21] we performed geometry optimizations of each junction using input structures with different dihedral angles (Figure S5).

In Figure 3b we plot illustrative optimized geometries for **Ph**-Au_1, **Cy**-Au_1, and **Xy**-Au_1, which support a qualitative rationalization of the measured conductance for these

https://doi.org/10.1021/acsphyschemau.5c00021
ACS Phys. Chem Au XXXX, XXX, XXX−XXX

junctions. For **Cy**, transport is through a sp^3-hybridized $n = 4$ backbone, providing a similar but lower conductance compared to **C4**. This conductance ordering may be rationalized given that the structural constraints of the cyclohexane group ensure the alkane chain between each linker cannot adopt a more conductive all-*trans* configuration,[22] and transmission through this cyclic hydrocarbon backbone may be further reduced through destructive σ-interference effects.[23] Transport through conjugated phenylene backbones may be expected to be more efficient than that through nonconjugated alkanes due to their smaller HOMO−LUMO gaps that better align frontier orbitals with the electrode Fermi level (E_F). However, we note that the geometry of the carboxylic acid linker in **Ph** orients the Au−O bond into the plane of the benzene group, *perpendicular* to the conjugated *p*-orbitals of the ring. This reduces electronic coupling between the delocalized backbone π-system and the electrode, forcing transport through the sp^2-hybridized σ-framework.[24] For **Xy** it is possible to access junction geometries that better align the terminal AuOC(O)− groups with the conjugated phenylene backbone, apparently providing a junction conductance comparable to those of **Ph** and **Cy** despite the longer, $n = 6$, conduction path.

We apply these and additional Au_1 cluster junctions to calculate tunnel couplings ($4t^2$), a metric that correlates well with experimental conductance.[25,26] For these neutral carboxylate-linked models, we obtain 2t from the energy difference between LUMO and LUMO+1 (see Computational Methods in the SI for justification), which provides the expected symmetric and antisymmetric orbital pair exhibiting Au *s*-O *p*-antibonding character (Figure 4a; analogous orbitals are provided for other junctions in Figure S7).[21] We validate our approach by plotting, in Figure 4b, $4t^2$ versus n for **C*n***-Au_1 models.[25] From a linear fit to these data, substituting $G = 4t^2$ into $G = G_c \cdot \exp(-\beta n)$, we obtain $\beta = 0.86/n$, in good agreement with our experimental result (Figure 2a). In Figure 4b, we also overlay the largest tunnel couplings obtained from all of the geometries evaluated for **Ph**-Au_1, **Cy**-Au_1, and **Xy**-Au_1 junctions (corresponding to the geometries in Figure 3b). While the tunnel coupling for each system is clearly dependent on its conformation (Table S4), the similarity of each of these maximum couplings to each other, and to the value found for **C4**-Au_1, supports our experimental finding that junctions formed from this series of molecules can exhibit a similar conductance. The potential energy landscapes of these junctions could be explored in future studies to evaluate the relative probabilities and thermal population of each conformation.

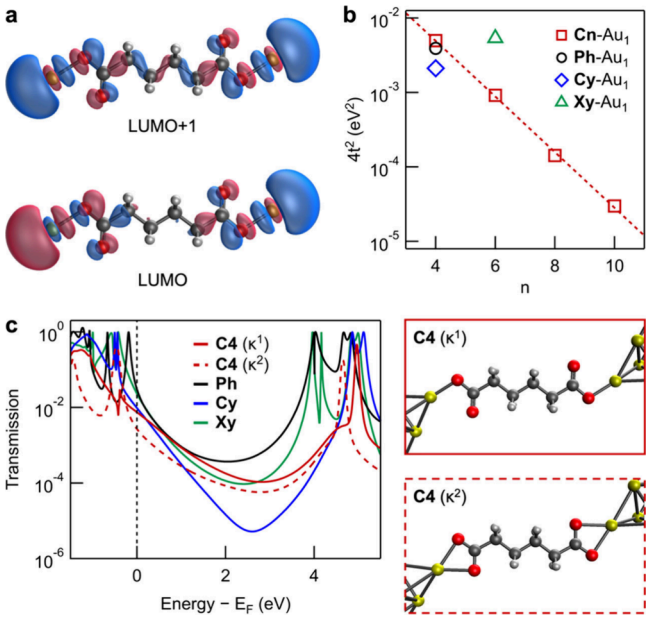

Figure 4. (a) Isosurface plots (isovalue of 0.06 Å^{-3}) of the tunnel-coupled LUMO and LUMO+1 orbitals for **C4**-Au_1. (b) A plot of the calculated tunnel couplings for **C*n***-Au_1 against n ($\beta = 0.86/n$), overlaid with the largest tunnel coupling for **Ph**-Au_1, **Cy**-Au_1, and **Xy**-Au_1 (all κ^1). (c) (Left) Overlaid transmission calculations for selected junctions, comprising the same (frozen) geometries used to calculate $4t^2$ in panel (b). (Right) The different contact geometries evaluated with **C4** junctions.

To further rationalize these findings, in Figure 4c we plot overlaid calculated transmission functions for **C4**, **Ph**, **Cy**, and **Xy** junctions with the same (frozen) geometries used to calculate $4t^2$ in Figure 4b. These quantum transport calculations are performed within the framework of DFT and the nonequilibrium Green's function (NEGF) formalism using FHI-aims[27] combined with the AITRANSS transport module (see the SI for additional details).[28−31] Our calculations support the conclusions obtained from the tunnel coupling analysis, with each junction exhibiting similar zero-bias conductance due to strong E_F pinning to the HOMO. In this sense, transport is dominated by weakly coupled occupied orbitals, and no significant midgap states[32] are observed for these chemisorbed Au−O contacts. Analogous calculations for fully relaxed junctions exhibit qualitatively similar features (see Figure S9 and the associated discussion). Interestingly, both tunnel coupling and transmission calculations reveal that the conductance of **C4** junctions varies by only a factor of 3−4 when both carboxylates are contacted through κ^1 or κ^2 coordination modes (Figure 4c and Tables S4 and S5), in agreement with previous studies focused on junctions with only a single carboxylate linker. We suggest that both modes are experimentally accessible and contribute, along with changes in the backbone geometry, to the width of the conductance peaks observed.

Independent of the precise coordination geometry, these linker groups are widely considered to bind in junctions as carboxylates ($-COO^-$).[3,7] The apparently spontaneous deprotonation of −COOH upon binding to gold is a process that is also important for thiols[33] and terminal alkynes,[34] although the larger pK_a of the alkyne C−H group may suggest a distinct deprotonation mechanism (pK_a^{DMSO}: $PhCO_2H$ = 11.1, PhSH = 10.31, PhCCH = 28.7).[35] Inspired by their plausible κ^1 coordination mode, we propose that carboxylic acids could be considered simply as −OH linkers comprising an acidic proton. While −OH groups have to date scarcely been explored as junction linkers, they may yet be widely utilized after deprotonation with an appropriate base (as recently reported for phenol)[36] or at a metal surface after incorporating adjacent chemical functionality that lowers their pK_a. Such contact chemistries could prove useful for forming junctions with oxophilic metal electrodes,[37] or to evaluate *in situ* chemical reactions thought to result in alkoxide-terminated junctions.[38]

Together, the results of this study motivate additional investigations using **IC** or related solvents to probe the properties of carboxylic acid-linked single-molecule junctions.

https://doi.org/10.1021/acsphyschemau.5c00021
ACS Phys. Chem Au XXXX, XXX, XXX−XXX

We note our approach may be expanded to characterize other families of compounds with polar or charged[36] backbones/contact groups. By substituting polar solvents with non-conducting analogues that can perform a similar solubilizing function, we greatly simplify STM-BJ experiments that typically otherwise require coated STM tips to minimize background electrochemical currents.[12] This may prove valuable for glovebox-based STM-BJ studies useful for investigations of air-sensitive electrode metals[38] and molecules,[39] in which the frequent use of coated STM tips would likely present a substantial experimental burden.

■ ASSOCIATED CONTENT

Supporting Information

The Supporting Information is available free of charge at https://pubs.acs.org/doi/10.1021/acsphyschemau.5c00021.

Additional experimental details and conductance and computational data (PDF)

■ AUTHOR INFORMATION

Corresponding Authors

María Camarasa-Gómez − *Centro de Física de Materiales (CFM-MPC) CSIC-UPV/EHU, 20018 Donostia-San Sebastián, Spain*; Email: maria.camarasa@ehu.eus

Daniel Hernangómez-Pérez − *CIC nanoGUNE BRTA, 20018 Donostia-San Sebastián, Spain*; orcid.org/0000-0002-4277-0236; Email: d.hernangomez@nanogune.eu

Michael S. Inkpen − *Department of Chemistry, University of Southern California, Los Angeles, California 90089, United States*; orcid.org/0000-0001-7339-8812; Email: inkpen@usc.edu

Authors

Clark Otey − *Department of Chemistry, University of Southern California, Los Angeles, California 90089, United States*

Mukund Sharma − *Department of Chemistry, University of Southern California, Los Angeles, California 90089, United States*

Jazmine Prana − *Department of Chemistry, University of Southern California, Los Angeles, California 90089, United States*

Thomas M. Czyszczon-Burton − *Department of Chemistry, University of Southern California, Los Angeles, California 90089, United States*

Alejandro Hernandez − *Department of Chemistry, University of Southern California, Los Angeles, California 90089, United States*

Complete contact information is available at: https://pubs.acs.org/10.1021/acsphyschemau.5c00021

Author Contributions

‖C.O. and M.S. contributed equally to this work.

Notes

The authors declare no competing financial interest.

■ ACKNOWLEDGMENTS

This work was primarily supported by University of Southern California (USC) startup funds and the National Science Foundation (NSF CAREER Award to M.S.I., CHE-2239614). A.H. thanks Agilent Technologies, and Steve and Cathy Gagliardi for their support of the USC-Cerritos Summer Internship in Sustainability program. M.C.-G. acknowledges support from the Diputación Foral de Gipuzkoa through Grant 2024-FELL-000007-01 and from the Gobierno Vasco-UPV/EHU Project No. IT1569-22. D.H.-P. is grateful for funding from the Diputación Foral de Gipuzkoa through Grants 2023-FELL-000002-01 and 2024-FELL-000009-01. D.H.-P. and M.C.-G. acknowledge the technical and human support provided by the DIPC Supercomputing Center.

■ REFERENCES

(1) Su, T. A.; Neupane, M.; Steigerwald, M. L.; Venkataraman, L.; Nuckolls, C. Chemical Principles of Single-Molecule Electronics. *Nature Rev. Mater.* **2016**, *1* (3), No. 16002.

(2) Huang, M.; Zhou, Q.; Liang, F.; Yu, L.; Xiao, B.; Li, Y.; Zhang, M.; Chen, Y.; He, J.; Xiao, S.; Chang, S. Detecting Individual Bond Switching within Amides in a Tunneling Junction. *Nano Lett.* **2021**, *21* (12), 5409−5414.

(3) Chen, F.; Li, X.; Hihath, J.; Huang, Z.; Tao, N. J. Effect of Anchoring Groups on Single-Molecule Conductance: Comparative Study of Thiol-, Amine-, and Carboxylic-Acid-Terminated Molecules. *J. Am. Chem. Soc.* **2006**, *128* (49), 15874−15881.

(4) Li, Z.; Smeu, M.; Ratner, M. A.; Borguet, E. Effect of Anchoring Groups on Single Molecule Charge Transport through Porphyrins. *J. Phys. Chem. C* **2013**, *117* (29), 14890−14898.

(5) Inkpen, M. S.; Leroux, Y. R.; Hapiot, P.; Campos, L. M.; Venkataraman, L. Reversible On-Surface Wiring of Resistive Circuits. *Chem. Sci.* **2017**, *8* (6), 4340−4346.

(6) Martín, S.; Haiss, W.; Higgins, S.; Cea, P.; López, M. C.; Nichols, R. J. A Comprehensive Study of the Single Molecule Conductance of α,ω-Dicarboxylic Acid-Terminated Alkanes. *J. Phys. Chem. C* **2008**, *112* (10), 3941−3948.

(7) Ahn, S.; Aradhya, S. V.; Klausen, R. S.; Capozzi, B.; Roy, X.; Steigerwald, M. L.; Nuckolls, C.; Venkataraman, L. Electronic Transport and Mechanical Stability of Carboxyl Linked Single-Molecule Junctions. *Phys. Chem. Chem. Phys.* **2012**, *14* (40), No. 13841.

(8) Gu, M.-W.; Peng, H. H.; Chen, I.-W. P.; Chen, C. Tuning Surface d Bands with Bimetallic Electrodes to Facilitate Electron Transport across Molecular Junctions. *Nat. Mater.* **2021**, *20* (5), 658−664.

(9) Zhou, X.-S.; Liang, J.-H.; Chen, Z.-B.; Mao, B.-W. An Electrochemical Jump-to-Contact STM-Break Junction Approach to Construct Single Molecular Junctions with Different Metallic Electrodes. *Electrochem. Commun.* **2011**, *13* (5), 407−410.

(10) Wang, Y.-H.; Hong, Z.-W.; Sun, Y.-Y.; Li, D.-F.; Han, D.; Zheng, J.-F.; Niu, Z.-J.; Zhou, X.-S. Tunneling Decay Constant of Alkanedicarboxylic Acids: Different Dependence on the Metal Electrodes between Air and Electrochemistry. *J. Phys. Chem. C* **2014**, *118* (32), 18756−18761.

(11) Li, P.; Ryder, M. R.; Stoddart, J. F. Hydrogen-Bonded Organic Frameworks: A Rising Class of Porous Molecular Materials. *Acc. Mater. Res.* **2020**, *1* (1), 77−87.

(12) Nagahara, L. A.; Thundat, T.; Lindsay, S. M. Preparation and Characterization of STM Tips for Electrochemical Studies. *Rev. Sci. Instrum.* **1989**, *60* (10), 3128−3130.

(13) Xu, B.; Tao, N. J. Measurement of Single-Molecule Resistance by Repeated Formation of Molecular Junctions. *Science* **2003**, *301* (5637), 1221−1223.

(14) Venkataraman, L.; Klare, J. E.; Tam, I. W.; Nuckolls, C.; Hybertsen, M. S.; Steigerwald, M. L. Single-Molecule Circuits with Well-Defined Molecular Conductance. *Nano Lett.* **2006**, *6* (3), 458−462.

(15) Quek, S. Y.; Kamenetska, M.; Steigerwald, M. L.; Choi, H. J.; Louie, S. G.; Hybertsen, M. S.; Neaton, J. B.; Venkataraman, L. Mechanically Controlled Binary Conductance Switching of a Single-Molecule Junction. *Nat. Nanotechnol.* **2009**, *4* (4), 230−234.

(16) Fatemi, V.; Kamenetska, M.; Neaton, J. B.; Venkataraman, L. Environmental Control of Single-Molecule Junction Transport. *Nano Lett.* **2011**, *11* (5), 1988−1992.
(17) Kim, L.; Czyszczon-Burton, T. M.; Nguyen, K. M.; Stukey, S.; Lazar, S.; Prana, J.; Miao, Z.; Park, S.; Chen, S. F.; Inkpen, M. S. Low Vapor Pressure Solvents for Single-Molecule Junction Measurements. *Nano Lett.* **2024**, *24* (32), 9998−10005.
(18) Park, Y. S.; Whalley, A. C.; Kamenetska, M.; Steigerwald, M. L.; Hybertsen, M. S.; Nuckolls, C.; Venkataraman, L. Contact Chemistry and Single-Molecule Conductance: A Comparison of Phosphines, Methyl Sulfides, and Amines. *J. Am. Chem. Soc.* **2007**, *129* (51), 15768−15769.
(19) Hong, Z.-W.; Aissa, M. A. B.; Peng, L.-L.; Xie, H.; Chen, D.-L.; Zheng, J.-F.; Shao, Y.; Zhou, X.-S.; Raouafi, N.; Niu, Z.-J. Quantum Interference Effect of Single-Molecule Conductance Influenced by Insertion of Different Alkyl Length. *Electrochem. Commun.* **2016**, *68*, 86−89.
(20) Grodzicki, A.; Łakomska, I.; Piszczek, P.; Szymańska, I.; Szłyk, E. Copper(I), Silver(I) and Gold(I) Carboxylate Complexes as Precursors in Chemical Vapour Deposition of Thin Metallic Films. *Coord. Chem. Rev.* **2005**, *249* (21−22), 2232−2258.
(21) Prana, J.; Kim, L.; Czyszczon-Burton, T.; Homann, G.; Chen, S.; Miao, Z.; Camarasa-Gomez, M.; Inkpen, M. Lewis-Acid Mediated Reactivity in Single-Molecule Junctions. *J. Am. Chem. Soc.* **2024**, *146* (48), 33265−33275.
(22) Jones, D. R.; Troisi, A. Single Molecule Conductance of Linear Dithioalkanes in the Liquid Phase: Apparently Activated Transport Due to Conformational Flexibility. *J. Phys. Chem. C* **2007**, *111* (39), 14567−14573.
(23) Zhang, B.; Garner, M. H.; Li, L.; Campos, L. M.; Solomon, G. C.; Venkataraman, L. Destructive Quantum Interference in Heterocyclic Alkanes: The Search for Ultra-Short Molecular Insulators. *Chem. Sci.* **2021**, *12* (30), 10299−10305.
(24) Cheng, Z. L.; Skouta, R.; Vazquez, H.; Widawsky, J. R.; Schneebeli, S.; Chen, W.; Hybertsen, M. S.; Breslow, R.; Venkataraman, L. In Situ Formation of Highly Conducting Covalent Au-C Contacts for Single-Molecule Junctions. *Nat. Nanotechnol.* **2011**, *6* (6), 353−357.
(25) Venkataraman, L.; Klare, J. E.; Nuckolls, C.; Hybertsen, M. S.; Steigerwald, M. L. Dependence of Single-Molecule Junction Conductance on Molecular Conformation. *Nature* **2006**, *442* (7105), 904−907.
(26) Nitzan, A. Electron Transmission through Molecules and Molecular Interfaces. *Annu. Rev. Phys. Chem.* **2001**, *52*, 681−750.
(27) Blum, V.; Gehrke, R.; Hanke, F.; Havu, P.; Havu, V.; Ren, X.; Reuter, K.; Scheffler, M. Ab Initio Molecular Simulations with Numeric Atom-Centered Orbitals. *Comput. Phys. Commun.* **2009**, *180* (11), 2175−2196.
(28) Camarasa-Gómez, M.; Hernangómez-Pérez, D.; Wilhelm, J.; Bagrets, A.; Evers, F. Molecular Transport. *arXiv* **2024**, No. 2411.01680.
(29) Arnold, A.; Weigend, F.; Evers, F. Quantum Chemistry Calculations for Molecules Coupled to Reservoirs: Formalism, Implementation, and Application to Benzenedithiol. *J. Chem. Phys.* **2007**, *126* (17), No. 174101.
(30) Bagrets, A. Spin-Polarized Electron Transport Across Metal−Organic Molecules: A Density Functional Theory Approach. *J. Chem. Theory Comput.* **2013**, *9* (6), 2801−2815.
(31) Camarasa-Gómez, M.; Hernangómez-Pérez, D.; Evers, F. Spin−Orbit Torque in Single-Molecule Junctions from Ab Initio. *J. Phys. Chem. Lett.* **2024**, *15* (21), 5747−5753.
(32) Li, C.; Pobelov, I.; Wandlowski, T.; Bagrets, A.; Arnold, A.; Evers, F. Charge Transport in Single Au | Alkanedithiol | Au Junctions: Coordination Geometries and Conformational Degrees of Freedom. *J. Am. Chem. Soc.* **2008**, *130* (1), 318−326.
(33) Bain, C. D.; Biebuyck, H. A.; Whitesides, G. M. Comparison of Self-Assembled Monolayers on Gold: Coadsorption of Thiols and Disulfides. *Langmuir* **1989**, *5* (3), 723−727.
(34) Millar, D.; Venkataraman, L.; Doerrer, L. H. Efficacy of Au−Au Contacts for Scanning Tunneling Microscopy Molecular Conductance Measurements. *J. Phys. Chem. C* **2007**, *111* (47), 17635−17639.
(35) Bordwell, F. G. Equilibrium Acidities in Dimethyl Sulfoxide Solution. *Acc. Chem. Res.* **1988**, *21* (12), 456−463.
(36) Lawson, B.; Skipper, H. E.; Kamenetska, M. Phenol Is a pH-Activated Linker to Gold: A Single Molecule Conductance Study. *Nanoscale* **2024**, *16* (4), 2022−2029.
(37) Kepp, K. P. A Quantitative Scale of Oxophilicity and Thiophilicity. *Inorg. Chem.* **2016**, *55* (18), 9461−9470.
(38) Czyszczon-Burton, T. M.; Montes, E.; Prana, J.; Lazar, S.; Rotthowe, N.; Chen, S. F.; Vázquez, H.; Inkpen, M. S. α,ω-Alkanedibromides Form Low Conductance Chemisorbed Junctions with Silver Electrodes. *J. Am. Chem. Soc.* **2024**, *146* (41), 28516−28526.
(39) Miao, Z.; Quainoo, T.; Czyszczon-Burton, T. M.; Rotthowe, N.; Parr, J. M.; Liu, Z.; Inkpen, M. S. Charge Transport across Dynamic Covalent Chemical Bridges. *Nano Lett.* **2022**, *22* (20), 8331−8338.

https://doi.org/10.1021/acsphyschemau.5c00021
ACS Phys. Chem Au XXXX, XXX, XXX−XXX